Second-order computational homogenization of heterogeneous materials with periodic microstructure

Andrea Bacigalupo, Luigi Gambarotta[1]

Department of Civil, Environmental and Architectural Engineering,
University of Genova,
Via Montallegro, 1 – 16145 Genova - Italy

Keywords: second-order continuum, computational homogenization, periodic microstructure, boundary layer effect, material characteristic length.

Abstract

A procedure for second-order computational homogenization of heterogeneous materials is derived from the unit cell homogenization, in which an appropriate representation of the micro-displacement field is assumed as the superposition of a local macroscopic displacement field, expressed in a polynomial form related to the macro-displacement field, and an unknown micro-fluctuation field accounting for the effects of the heterogeneities. This second contribution is represented as the superposition of two unknown functions each of which related to the first-order and to the second-order strain, respectively. This kinematical micro-macro framework guarantees that the micro-displacement field is continuous across the interfaces between adjacent unit cells and implies a computationally efficient procedure that applies in two steps. The first step corresponds to the standard homogenization, while the second step is based on the results of the first step and completes the second-order homogenization.

Two multi-phase composites, a three-phase and a laminated composite, are analysed in the examples to assess the reliability of the homogenization techniques. The computational homogenization is carried out by a FE analysis of the unit cell; the overall elastic moduli and the characteristic lengths of the second-order equivalent continuum model are obtained. Finally, the simple shear of a constrained heterogeneous two-dimensional strip made up of the composites considered is analysed by considering a heterogeneous continuum and a

[1] Corresponding author, gambarotta@dicat.unige.it

homogenized second-order continuum; the corresponding results are compared and discussed in order to identify the validity limits of the proposed technique.

1. Introduction

First-order or local homogenization techniques have long been applied to obtain the constitutive equations of heterogeneous materials. Although such procedures allow one to incorporate the presence of the underlying microstructure in the constitutive equations, the fundamental assumption that the microstructural length scale is infinitely small compared to the characteristic macrostructural size may present strong validity limits. In fact, this condition is never reached because the microstructure size does not equal zero and may be comparable with the characteristic size of the macrocomponent or with the length scale associated with the macroscopic spatial variability in the loading. A condition that determines different types of size effects or zones of highly localized deformation which cannot be described by a first-order continuum model.

Non-local or generalized continua allow one to introduce length scales into the constitutive equation and hence to account for the above size effects. In this context, the problem of deriving the constitutive equations and the corresponding length scales from the underlying microstructure through non-local homogenization techniques seems to be important. Special attention is paid here to materials having periodic microstructure, for which it is possible to identify a periodic unit cell representative of the material itself.

Higher-order constitutive equations for periodic, linear elastic heterogeneous materials, whereby all microstructural constituents are treated as a classical continuum, have been deduced in [1-5]. A computational procedure has been developed in [5] and applied to the homogenization of a periodic matrix-inclusion composite. Although the asymptotic solution techniques provide a mathematically rigorous tool of higher-order homogenization, as observed in [5], they seem to be computationally burdensome in comparison to the methods based on the computational homogenization of the unit cell developed for Cosserat homogenization [6-8], couple-stress homogenization [9-11] and second-order homogenization [12-14]. In these methods the kinematics at the micro and at the macro-scale in the unit cell are described by developing the microscopic displacement field as the superposition of a local macroscopic displacement field, assumed in a polynomial form related to the macro-displacement field, and an unknown micro-displacement fluctuation field accounting for the effects of the heterogeneities. The calculations of strain and stress

distributions inside the unit cell and the subsequent ensemble averaging are performed by imposing properly prescribed displacements on the unit cell boundaries. However, while in the first order homogenization the condition of continuity of the local fields at the interface of adjacent cells results in a condition of periodicity of the micro-displacement fluctuation field in the unit cell, in the second-order homogenization the prescription of essential boundary conditions appears to be a more complex problem. In [9], [7], [10-11] the micro-displacement fluctuation field is assumed vanishing on the boundary of the unit cell, while in [12] the condition of periodicity of the micro-fluctuation field is extended in a generalized sense that includes the average of the micro-fluctuation field itself on the unit cell sides. In [13] an extension of this approach has been proposed to encompass not only periodic-type boundary conditions for the unit cell but also traction and displacement boundary conditions in a generalized unified manner. However, unlike the standard homogenization, the micro-displacement field obtained from the mentioned approaches in case of prescribed homogeneous second-order strain results to be discontinuous across the interface between adjacent cells, a circumstance that is also observed in the microscopic stress field.

The second-order computational homogenization of heterogeneous media presented in this paper is derived by considering an appropriate representation of the micro-displacement fluctuation field to superimpose on the polynomial displacement field. According to this representation, already proposed by [14], the micro-displacement fluctuation field is assumed as the superposition of two unknown functions each of them related to the first-order and to the second-order strain, respectively. This kinematical micro-macro framework guarantees that the micro-displacement field is continuous across the interfaces between adjacent unit cells and implies a computationally efficient procedure that applies in two steps. The first step corresponds to the standard homogenization, while the second step is based on the results of the first step and completes the second-order homogenization.

To assess the reliability of the homogenization techniques two multi-phase composites are considered in the examples. The first is a three-phase composite with a multilayered microstructure and the second is a laminated composite. The computational homogenizations are carried out by a FE analysis of the unit cell and the overall elastic moduli and the characteristic lengths of the second-order equivalent continuum model are obtained. Finally, the simple shear of a constrained heterogeneous two-dimensional strip

made up of the considered composites is analysed by considering a heterogeneous continuum and a homogenized second-order continuum; the corresponding results are compared and discussed in order to identify the validity limits of the proposed technique.

2. Basic relations for second gradient continua

Let us consider a deformable continuum body $\mathcal{B}$ with boundary $\partial\mathcal{B}$, $\mathbf{y}$ the position vector of a material point with respect to the origin O. The displacement vector at $\mathbf{y}$ is $\mathbf{U}(\mathbf{y})$, having component U_i with respect to an assumed orthonormal basis $(\mathbf{e}_i,\ i=1,2,3)$; small displacements are considered. The displacement gradient is denoted by $\mathbf{H}(\mathbf{y})=\nabla_{\mathrm{y}}\mathbf{U}(\mathbf{y})$ and, according to Germain [15], the strain field in the second gradient continuum is represented by the symmetric first-order strain tensor $\mathbf{E}(\mathbf{y})=sym\nabla_{\mathrm{y}}\mathbf{U}(\mathbf{y})$, having components $E_{ij}=E_{ji}$, and by the second-order strain tensor $\boldsymbol{\kappa}(\mathbf{y})=\nabla_{\mathrm{y}}\otimes\nabla_{\mathrm{y}}\mathbf{U}(\mathbf{y})$, which is a third-order tensor having components $\kappa_{ijk}=\kappa_{ikj}$ symmetric with respect to j and k. Moreover, the mean rotation tensor at $\mathbf{y}$ is represented by the second-order tensor $\boldsymbol{\Omega}(\mathbf{y})=skw\nabla_{\mathrm{y}}\mathbf{U}(\mathbf{y})$.

The stress field is described by the symmetric first-order stress tensor $\boldsymbol{\Sigma}(\mathbf{y})$ ($\Sigma_{ij}=\Sigma_{ji}$) and the second-order stress tensor $\boldsymbol{\mu}(\mathbf{y})$ (third-order tensor having components $\mu_{ijk}=\mu_{ikj}$ symmetric with respect to j and k). From these stress tensors the real stress is defined as $\mathbf{T}(\mathbf{y})=\boldsymbol{\Sigma}(\mathbf{y})-Div_{\mathrm{y}}\boldsymbol{\mu}(\mathbf{y})$ (in components $\mathrm{T}_{ij}=\Sigma_{ij}-\mu_{ijk,k}$) so that, in general, $\mathbf{T}(\mathbf{y})$ is not symmetric. The equilibrium equation in the domain $\mathcal{B}$ is expressed in the form

$$Div_{\mathrm{y}}\left(\boldsymbol{\Sigma}(\mathbf{y})-Div_{\mathrm{y}}\boldsymbol{\mu}(\mathbf{y})\right)+\mathbf{f}=\mathbf{0},\qquad \left(\Sigma_{ij,j}-\mu_{ijk,jk}+f_i=0\right), \tag{1}$$

$\mathbf{f}$ being the body force.

The first-order and second-order stress tensors are conjugate to the corresponding strain tensors so that the power of the internal forces is written in the form

$$\mathcal{P}=\int_{\mathcal{B}}\left(\boldsymbol{\Sigma}:\dot{\mathbf{E}}+\boldsymbol{\mu}\vdots\dot{\boldsymbol{\kappa}}\right)da\,, \tag{2}$$

where $\dot{\mathbf{E}}$ and $\dot{\boldsymbol{\kappa}}$ are the rates of the strain tensors. Accordingly, the constitutive equations in case of linear elasticity take the form

$$\begin{aligned}\boldsymbol{\Sigma} &= \mathbb{C}\mathbf{E} + \mathbb{Y}\boldsymbol{\kappa},\\ \boldsymbol{\mu} &= \mathbb{Y}^{\mathrm{T}}\mathbf{E} + \mathbb{S}\boldsymbol{\kappa},\end{aligned} \tag{3}$$

$\mathbb{C}$ being the (standard) fourth-order elasticity tensor which is associated with the local continuum, $\mathbb{S}$ the sixth order tensor related to second-order stress and strain tensors and $\mathbb{Y}$ a fifth order tensor taking into account the coupling between the first and second-order stress and strain tensors.

3. Multiscale kinematic for materials with periodic microstructure

Let us consider a heterogeneous elastic medium occupying a planar domain having a microstructure periodically distributed, as shown in figure 1.a, i.e. the elasticity tensor $\mathbb{C}^m$ is periodic. This composite is analysed at the micro-scale as a Cauchy continuum. At the material point $\mathbf{x}$ of the heterogeneous elastic medium the micro-displacement $\mathbf{u}(\mathbf{x})$ is considered together with the corresponding micro-strain tensor $\boldsymbol{\varepsilon}(\mathbf{x})=sym\nabla_{\mathbf{x}}\mathbf{u}$ and micro-stress tensor $\boldsymbol{\sigma}(\mathbf{x})$. The mechanical behaviour of the composite can be analysed on the basis of the smallest repeatable element, namely a representative unit cell occupying the planar region $\mathscr{A}(\mathbf{y})$ having its centre in $\mathbf{y}$ (see figure 1.b). As shown in figure 1.b the unit cell may be represented by two independent vectors of periodicity $\mathbf{v}_1$, $\mathbf{v}_2$, assumed orthogonal here, so that the boundary C of the unit cell is made up of two pairs of opposite sides corresponding to each other by means of a translation along $\mathbf{v}_1$ or $\mathbf{v}_2$. According to this representation, a variable is periodic in the unit cell $\mathscr{A}$, or $\mathscr{A}$-periodic, if it takes identical values at two points on the boundary of the unit cell whose difference is a vector of periodicity. The position $\mathbf{x}$ of a point in the composite may be expressed by its relative position vector $\mathbf{z}=\mathbf{x}-\mathbf{y}$ with respect to the position $\mathbf{y}$ of the unit cell in which $\mathbf{x}$ is located.

In order to couple the classical continuum at the micro-scale to the second-order continuum at the macro-scale, the micro-displacement field in the unit cell may be expressed in the form $\mathbf{u}(\mathbf{x})=\mathbf{u}(\mathbf{y},\mathbf{z})$ highlighting the dependence on the unit cell position $\mathbf{y}$, the macro-position, and on the local position $\mathbf{z}$ at a point of interest. According to [9], [7], [13], [14] the displacement field is assumed as the superposition

$$\mathbf{u}(\mathbf{y},\mathbf{z})=\mathbf{u}^{*}(\mathbf{y},\mathbf{z})+\tilde{\mathbf{u}}(\mathbf{y},\mathbf{z}), \tag{4}$$

of a polynomial function depending on the macro-displacement and macro-strain components at $\mathbf{y}$

$$\mathbf{u}^*(\mathbf{y},\mathbf{z}) = \mathbf{U}(\mathbf{y}) + \mathbf{H}(\mathbf{y})\mathbf{z} + \frac{1}{2}\boldsymbol{\kappa}(\mathbf{y}):(\mathbf{z}\otimes\mathbf{z}), \tag{5}$$

and a complementary displacement field $\tilde{\mathbf{u}}(\mathbf{y},\mathbf{z})$ that represents the microstructural displacement fluctuation field considered here to account for the microscale contribution due to the presence of the heterogeneities. In particular, the polynomial function (5) can be considered as a 2nd degree Taylor polynomial of the displacement vector about the unit cell centre $\mathbf{y}$.

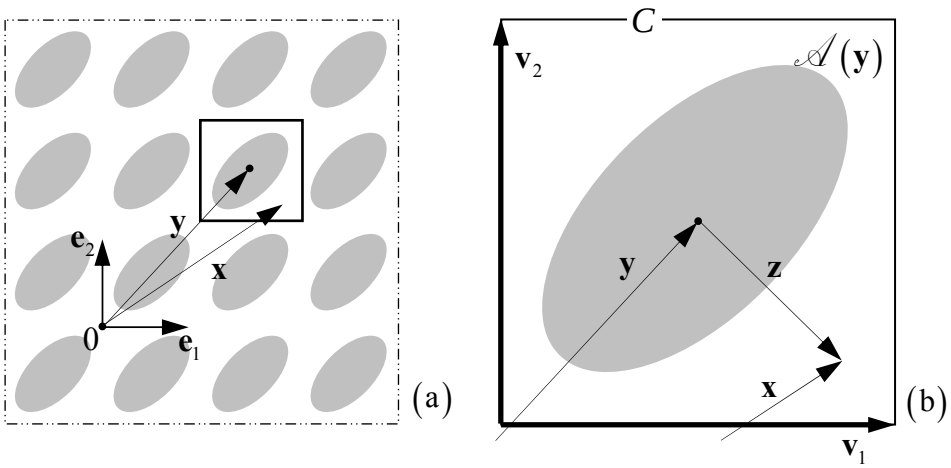

Fig. 1 (a) Periodic composite; (b) Unit cell and periodicity vectors.

When carrying out a first-order homogenization of a heterogeneous material a homogeneous macro-displacement gradient is considered in the body. The micro-displacement field (4) is obtained by imposing the $\mathcal{A}$-periodicity condition on the micro-displacement fluctuation, i.e.

$$\tilde{\mathbf{u}}(\mathbf{y},\mathbf{z}_b) = \tilde{\mathbf{u}}(\mathbf{y},\mathbf{z}_b + \mathbf{v}_i), \quad \forall \mathbf{z}_b \in C_i,\ i = 1,2, \tag{6}$$

where $\mathbf{z}_b$ is the local position vector at a point on the boundary, $C_i,\ i = 1,2$ (see figure 2). This condition, therefore, guarantees the compatibility of the displacement field in the body, i.e. the continuity of the micro-displacement on the cell interfaces. From equation (6) the micro-displacement field is obtained by numerically solving the elasticity problem of the unit cell with boundary conditions prescribed on the relative micro-displacement field

$$\mathbf{u}(\mathbf{y},\mathbf{z}_b + \mathbf{v}_i) - \mathbf{u}(\mathbf{y},\mathbf{z}_b) = \mathbf{u}^*(\mathbf{y},\mathbf{z}_b + \mathbf{v}_i) - \mathbf{u}^*(\mathbf{y},\mathbf{z}_b), \quad \forall \mathbf{z}_b \in C_i,\ i = 1,2, \tag{7}$$

where the r.h.s. in equation (7) depends on the strain components according to equation (5).

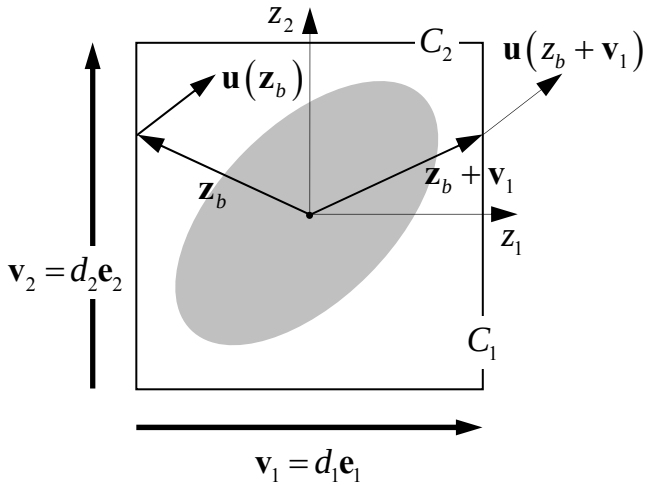

Fig. 2 Displacement vectors of points at the boundary of the unit cell.

When considering the second-order homogenization, the second-order strain tensor $\boldsymbol{\kappa}(\mathbf{y}) = \nabla_{\mathrm{y}} \otimes \mathbf{H}(\mathbf{y})$ is assumed homogeneous in the body at the macro-scale, so that the gradient tensor $\mathbf{H}(\mathbf{y})$ turns out to be affine in the body. In this case, the $\mathscr{A}$-periodicity condition (6) is not sufficient to guarantee the continuity of the micro-displacement field in the heterogeneous body at points on the unit cell boundaries and to formulate boundary conditions on the unit cell which are useful to evaluate the micro-displacement field. To overcome this second problem different conditions have been proposed to supplement the condition of $\mathscr{A}$-periodicity on the micro-displacement fluctuation. In [12] the condition of vanishing average fluctuation displacement on the edges of the unit cell was put forward, while in [13] an integral condition on the unit cell boundary was proposed based on a proper definition of the second-order strain tensor in terms of the micro-displacement field. Other approaches [9-11], [7] simply consider the fluctuation displacement field vanishing on the unit cell boundary. In any case the problem of inter-element displacement continuity seems to be open.

To obtain continuous displacement fields across the unit cell interfaces let us consider the fluctuation field split into two vector functions:

$$\tilde{\mathbf{u}}(\mathbf{y},\mathbf{z}) = \mathbf{r}^1(\mathbf{y},\mathbf{z}) + \mathbf{r}^2(\mathbf{y},\mathbf{z}), \tag{8}$$

each of them having the following representation in components

$$r_i^1(\mathbf{y},\mathbf{z}) = \theta_{ikl}^1(\mathbf{z})\left[H_{kl}(\mathbf{y}) + \kappa_{klp}(\mathbf{y})z_p\right],$$
$$r_i^2(\mathbf{y},\mathbf{z}) = \theta_{iklp}^2(\mathbf{z})\kappa_{klp}(\mathbf{y}). \tag{9}$$

In representation (9), that was first proposed in [14], the unknown functions $\theta_{ikl}^1(\mathbf{z})$ and $\theta_{iklp}^2(\mathbf{z})$ are the components of a third-order tensor $\boldsymbol{\Theta}^1(\mathbf{z})$ and a fourth order tensor $\boldsymbol{\Theta}^2(\mathbf{z})$, respectively, and must be selected in order to satisfy the micro-displacement continuity at the interfaces of adjacent unit cells. Let us consider the micro-displacement on a cell $\mathscr{A}(\mathbf{y}_0)$ centred on $\mathbf{y}_0$ in the case of homogeneous second-order strain field $\boldsymbol{\kappa}$ at the macro-scale; at $\mathbf{y}_0$ the macro-displacement $\mathbf{U}(\mathbf{y}_0)$ and its gradient $\mathbf{H}(\mathbf{y}_0)$ are assumed to be known. At a point on the boundary C_i (i=1,2) shown in figure 3 the micro-displacement is obtained by equations (4), (5) and (8), (9)

$$\mathbf{u}(\mathbf{y}_0,\mathbf{z}_0^i) = \mathbf{U}(\mathbf{y}_0) + \mathbf{H}(\mathbf{y}_0)\mathbf{z}_0^i + \frac{1}{2}\boldsymbol{\kappa}:(\mathbf{z}_0^i \otimes \mathbf{z}_0^i) + \boldsymbol{\Theta}^1(\mathbf{z}_0^i):\left[\mathbf{H}(\mathbf{y}_0) + \boldsymbol{\kappa}\mathbf{z}_0^i\right] + \boldsymbol{\Theta}^2(\mathbf{z}_0^i)\vdots\boldsymbol{\kappa}; \tag{10}$$

the displacement of the corresponding point on the adjacent unit cell $\mathscr{A}(\mathbf{y}_i)$ is:

$$\mathbf{u}(\mathbf{y}_i,\mathbf{z}_i) = \mathbf{U}(\mathbf{y}_i) + \mathbf{H}(\mathbf{y}_i)\mathbf{z}_i + \frac{1}{2}\boldsymbol{\kappa}:(\mathbf{z}_i \otimes \mathbf{z}_i) + \boldsymbol{\Theta}^1(\mathbf{z}_i):\left[\mathbf{H}(\mathbf{y}_i) + \boldsymbol{\kappa}\mathbf{z}_i\right] + \boldsymbol{\Theta}^2(\mathbf{z}_i)\vdots\boldsymbol{\kappa}. \tag{11}$$

For a given displacement and a displacement gradient at the cell $\mathbf{y}_0$ (see figure 3) the corresponding quantities at the adjacent cells are $\mathbf{U}(\mathbf{y}_i) = \mathbf{U}(\mathbf{y}_0) + \mathbf{H}(\mathbf{y}_0)\mathbf{v}_i + \frac{1}{2}\boldsymbol{\kappa}:(\mathbf{v}_i \otimes \mathbf{v}_i)$, $\mathbf{H}(\mathbf{y}_i) = \mathbf{H}(\mathbf{y}_0) + \boldsymbol{\kappa}\mathbf{v}_i$, respectively, and the equation (11) may be rewritten in the form:

$$\begin{aligned}\mathbf{u}(\mathbf{y}_i,\mathbf{z}_i) = \mathbf{U}(\mathbf{y}_0) + \mathbf{H}(\mathbf{y}_0)\left[\mathbf{v}_i + \mathbf{z}_i\right] + \frac{1}{2}\boldsymbol{\kappa}:\left[(\mathbf{v}_i + \mathbf{z}_i)\otimes(\mathbf{v}_i + \mathbf{z}_i)\right] + \\ + \boldsymbol{\Theta}^1(\mathbf{z}_i):\left[\mathbf{H}(\mathbf{y}_0) + \boldsymbol{\kappa}(\mathbf{v}_i + \mathbf{z}_i)\right] + \boldsymbol{\Theta}^2(\mathbf{z}_i)\vdots\boldsymbol{\kappa}.\end{aligned} \tag{12}$$

By noting from figure 3 that $\mathbf{z}_0^i = \mathbf{v}_i + \mathbf{z}_i$ and after imposing the continuity of the micro-displacement field $\mathbf{u}(\mathbf{y}_0,\mathbf{z}_0^i) = \mathbf{u}(\mathbf{y}_1,\mathbf{z}_i)$ at the boundaries C_i (i=1,2) of the adjacent unit cells one obtains the condition of $\mathscr{A}$-periodicity for the unknown functions

$$\begin{aligned}&\boldsymbol{\Theta}^1(\mathbf{z}_0^i) = \boldsymbol{\Theta}^1(\mathbf{z}_i) = \boldsymbol{\Theta}^1(\mathbf{z}_0^i - \mathbf{v}_i) \\ &\boldsymbol{\Theta}^2(\mathbf{z}_0^i) = \boldsymbol{\Theta}^2(\mathbf{z}_i) = \boldsymbol{\Theta}^2(\mathbf{z}_0^i - \mathbf{v}_i)\end{aligned} \qquad \mathbf{z}_0^i \in C_i, \quad i=1,2, \tag{13}$$

which will be applied below to obtain the microscopic displacement field in the unit cell, as shown in Section 4.

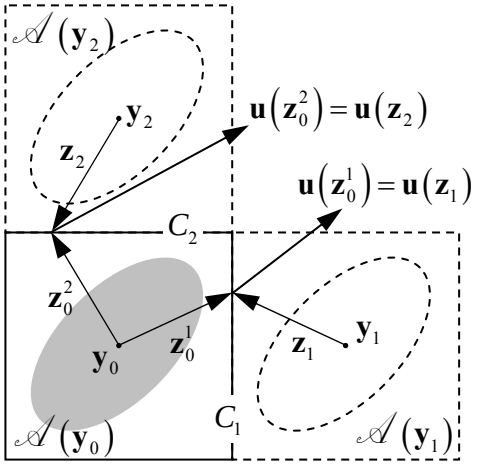

Fig. 3 Displacement vectors at points on boundaries of adjacent cells.

The components of the macro-scale displacement and strain fields can be related with the micro-displacement field in the unit cell centered on $\mathbf{y}$ through proper averages of the local fields over the unit cell. By averaging the micro-displacement field obtained from equations (4), (5), (8), (9), the components of the macro-displacement are obtained in terms of the average of the micro-displacement component, the macro-displacement gradient and the higher-order strain

$$U_i = \left\langle u_i \right\rangle_{\mathbf{y}} - \frac{1}{2A} \mathrm{J}_{pp} \kappa_{ipp} - \left\langle \theta^1_{ikl} \right\rangle_{\mathbf{y}} H_{kl} - \left\langle \theta^1_{ikl} z_p \right\rangle_{\mathbf{y}} \kappa_{klp} - \left\langle \theta^2_{iklp} \right\rangle_{\mathbf{y}} \kappa_{klp}, \tag{14}$$

where the symbol $\left\langle \bullet \right\rangle_{\mathbf{y}}$ represents the average of the considered function over the unit cell centred on $\mathbf{y}$, A is the area of the unit cell, $\mathrm{J}_{pp} = \int_A z_p^2 \mathrm{d}a$ is the moment of inertia of the cell. It is worth noting that in case of a centro-symmetric unit cell ($\mathbb{C}^m(\mathbf{z}) = \mathbb{C}^m(-\mathbf{z})$) one obtains $\left\langle \theta^1_{ikl} \right\rangle_{\mathrm{y}} = 0$. Moreover, the components of the macro-displacement gradient tensor are obtained by averaging the micro-displacement gradient

$$H_{kl} = \left\langle u_{k,l} \right\rangle_{\mathbf{y}} - \mathrm{M}^1_{krqpl} \kappa_{rqp}, \tag{15}$$

where the term $\mathrm{M}^1_{iklrq} = \int_C \theta^1_{ikl} z_r n_q ds$ is vanishing in case of a centro-symmetric cell as a consequence of the periodicity condition (13). Finally, from the averaging of the quantity

$\frac{1}{2}\left\langle u_{i,q}z_r + u_{i,r}z_q \right\rangle_{\mathbf{y}}$ the components of the second-order strain are expressed in a linear system of equation in the form

$$\begin{aligned}&\frac{1}{2}\left(\mathrm{J}_{rr}+\mathrm{J}_{qq}\right)\left(\kappa_{irq}+\kappa_{iqr}\right)-\delta_{rq}\mathrm{J}_{pp}\kappa_{ipp}+\mathrm{N}^{1}_{iklprq}\kappa_{klp}+\mathrm{M}^{2}_{iklprq}\kappa_{klp}=\\&\quad=-\mathrm{M}^{1}_{ikl(rq)}H_{kl}-2A\delta_{rq}U_i+\int_C u_i\left(z_r n_q+z_q n_r\right)\mathrm{d}s,\end{aligned}\tag{16}$$

where the symmetric part of M^{1}_{iklrq} is considered $\mathrm{M}^{1}_{ikl(rq)}=\int_C \theta^{1}_{ikl}\left(z_r n_q+z_q n_r\right)ds$ and the terms $\mathrm{M}^{2}_{iklprq}=\int_C \theta^{1}_{ikl}z_p\left(z_r n_q+z_q n_r\right)ds$ and $\mathrm{N}^{1}_{iklprq}=\int_C \theta^{2}_{iklp}\left(z_r n_q+z_q n_r\right)ds$ are introduced. In the system of linear equations (14), (15) and (16) the unknowns U_i, H_{ij}, κ_{ijh} linearly depend on proper averages over the unit cell of the micro-displacement $\mathbf{u}(\bullet)$ or, equivalently, of the functions $\boldsymbol{\Theta}^{1}(\bullet)$, $\boldsymbol{\Theta}^{2}(\bullet)$. By substituting equations (14) and (15) in (16) and after simple manipulations one obtains the system of linear equations

$$\frac{1}{2}\left(\mathrm{J}_{rr}+\mathrm{J}_{qq}\right)\left(\kappa_{irq}+\kappa_{iqr}\right)+F^{1}_{iklprq}\kappa_{klp}=-F^{2}_{irq}\tag{17}$$

with the components of the second-order strain unknown and having defined

$$\begin{aligned}F^{1}_{iklprq}&=\mathrm{N}^{1}_{iklprq}+\mathrm{M}^{2}_{iklprq}-\mathrm{M}^{1}_{ist(rq)}\mathrm{M}^{1}_{sklpt}-2\delta_{rq}\delta_{ik}\delta_{lp}\mathrm{J}_{lp}+\\&\quad-2A\delta_{rq}\left(\left\langle\theta^{1}_{ikl}z_p\right\rangle_{\mathbf{y}}+\left\langle\theta^{2}_{iklp}\right\rangle_{\mathbf{y}}-\left\langle\theta^{1}_{ist}\right\rangle_{\mathbf{y}}\mathrm{M}^{1}_{sklpt}\right),\\F^{2}_{irq}&=\mathrm{M}^{1}_{ikl(rq)}\left\langle u_{k,l}\right\rangle_{\mathbf{y}}+2A\delta_{rq}\left(\left\langle u_i\right\rangle_{\mathbf{y}}-\left\langle\theta^{1}_{ikl}\right\rangle_{\mathbf{y}}\left\langle u_{k,l}\right\rangle_{\mathbf{y}}\right).\end{aligned}\tag{18}$$

Given the symmetry of the components N^{1}_{iklprq} and M^{2}_{iklprq} with respect to the indexes *r* and *q*, even the components of the tensors $\mathbf{F}^{1}$ and $\mathbf{F}^{2}$ in equation (18) retain such a property, i.e. $F^{1}_{iklprq}=F^{1}_{iklpqr}$, $F^{2}_{irq}=F^{2}_{iqr}$. As a consequence, the components of the second-order strain obtained by solving (17) turn out to be symmetric with respect to the same indexes $\kappa_{irq}=\kappa_{iqr}$. Lastly, this procedure ends with the evaluation through equations (14) and (15) of the macro-displacement and the second-order strain, respectively.

While the conditions of $\mathcal{A}$-periodicity (13) ensure the continuity of displacement, it is not so for the tractions at the interface between adjacent unit cells. According to equations

(4), (5), (8) and (9), for arbitrary macro strain tensors **H** and $\boldsymbol{\kappa}$ the micro-stress components in the unit cell at **y** take the following form

$$\sigma_{rs} = \left(C^m_{rsiq} + C^m_{rsjp}\theta^1_{jiq,p}\right)H_{iq} + \left(C^m_{rsiq}\theta^2_{ijpl,q} + C^m_{rsjp}z_l + C^m_{rsiq}\theta^1_{ijp,q}z_l + C^m_{rsil}\theta^1_{ijp}\right)\kappa_{jpl}, \quad (19)$$

C^m_{rsip} being the component of the local elasticity tensor $\mathbb{C}^m$ here assumed smooth at the cell interfaces. By imposing the equilibrium equation in the unit cell with vanishing body forces $\sigma_{rs,s} = \partial\sigma_{rs}/\partial z_s = 0$ for arbitrary macro-strain ($\forall\, H_{iq},\ \kappa_{jpl}$) two systems of PDEs with the unknown functions θ^1_{ijp} and θ^2_{ijpl} are obtained

$$\begin{aligned} &C^m_{rsiq,s} + \left(C^m_{rsjp}\theta^1_{jiq,p}\right)_{,s} = 0, \\ &\left(C^m_{rsiq}\theta^2_{ijpl,q}\right)_{,s} + \left(C^m_{rsjp}z_l\right)_{,s} + \left(C^m_{rsiq}\theta^1_{ijp,q}z_l\right)_{,s} + \left(C^m_{rsil}\theta^1_{ijp}\right)_{,s} = 0. \end{aligned} \quad (20)$$

The solution θ^1_{ijp} of equation (20.1) with periodic boundary conditions (13.1) can be obtained up to an arbitrary constant, that may be fixed by the normalized condition $\left\langle\theta^1_{ijp}\right\rangle_{\mathbf{y}} = 0$. As a consequence, the first-order elasticity tensor of the homogenized medium may be evaluated as $C^1_{rsip} = \left\langle C^m_{rsip} + C^m_{rsiq}\theta^1_{ijp,q}\right\rangle_{\mathbf{y}}$ (see [14]). The functions θ^2_{ijpl} are obtained by solving equation (20.2) with periodic boundary conditions (13.2). If these functions are repeated in the tessellation of the unit cells, thereby obtaining a periodic prolongation along the periodicity vectors, two continuous $\mathcal{A}$-periodic functions are obtained. Unlike functions θ^1_{ijp}, functions θ^2_{ijpl} are not differentiable at a point on the interface of adjacent unit cells ($\theta^2_{ijpl} \in C^0$ at the boundaries C_i, i=1,2). In particular, at points on the unit cell boundary the normal derivative of the function θ^2_{ijpl} is not defined (in the ordinary sense) because it is discontinuous: a characteristic that follows from equation (20.2). In fact, by averaging both the terms in equation (20.2) one obtains

$$\begin{aligned} \left\langle\left(C^m_{rsiq}\theta^2_{ijpl,q}\right)_{,s}\right\rangle_{\mathbf{y}} &= -\left\langle\left(C^m_{rsjp}z_l\right)_{,s} + \left(C^m_{rsiq}\theta^1_{ijp,q}z_l\right)_{,s} + \left(C^m_{rsil}\theta^1_{ijp}\right)_{,s}\right\rangle_{\mathbf{y}} = \\ &= -C^1_{rljp} - \left\langle C^m_{rsjp,s}z_l + \left(C^m_{rsiq}\theta^1_{ijp,q}\right)_{,s}z_l\right\rangle_{\mathbf{y}} \neq 0 \end{aligned} \quad . \quad (21)$$

while if the gradient $\theta^2_{ijpl,q}$ was a continuous function the r.h.s. of equation (21) would be zero (see [1]). Consequently, the components of the micro-stress tensor given by equation (19) are also discontinuous at points on the interfaces of adjacent unit cells. In conclusion,

this approach has the advantage of obtaining compatible micro-displacement fields, although the corresponding stress fields satisfy the equilibrium in the unit cells but not at the cell interfaces.

4. Second-order homogenization

The multi-scale kinematics assumed in the previous Section with the representation of the micro-displacement fluctuation field given in equations (8) and (9) are the key points on which the two-step computational homogenization is based.

The first step is the standard first-order homogenization. The unknown function $\boldsymbol{\Theta}^1(\mathbf{z})$, whose component $\theta^1_{ikl}(\mathbf{z})$ represents the fluctuation displacement along direction $\mathbf{e}_i$ associated to the component H_{kl} of the macro-displacement gradient, is obtained by the standard computational analysis of the unit cell with prescribed periodic boundary conditions (7) on the micro-displacement field. Once the micro-displacement $\mathbf{u}(\mathbf{y},\mathbf{z})$ in the unit cell $\mathcal{A}(\mathbf{y})$ is obtained, the 2^3 unknown functions θ^1_{ijk} are derived by applying equation (10) for vanishing $\mathbf{U}(\mathbf{y})$ and $\boldsymbol{\kappa}$, i.e. by solving the system of linear equations $H_{jk}(\mathbf{y})\theta^1_{ijk}(\mathbf{z}) = u_i(\mathbf{y},\mathbf{z}) - H_{ij}(\mathbf{y})z_j$. At this stage the overall (Cauchy) elasticity tensor $\mathbb{C}$ may be evaluated, which maps the macro-strain tensor $\mathbf{E}$ to the macro-stress tensor $\boldsymbol{\Sigma}$.

The second step is carried out by considering a homogeneous second-order strain field and vanishing macro-strain $\mathbf{E} = \mathbf{0}$. The 2^4 unknown functions $\theta^2_{ijkl}(\mathbf{z})$ are obtained by analysing the unit cell with prescribed boundary conditions on the micro-displacement field derived from the $\mathcal{A}$-periodicity condition (13.2). For an arbitrary prescribed second-order strain tensor $\boldsymbol{\kappa}$, the micro-displacement $\mathbf{u}^{II}(\mathbf{y},\mathbf{z})$ is written at corresponding points on the boundary $\mathbf{z}_b$ and $\mathbf{z}_b + \mathbf{v}_i$ according to equation (10) and then the condition of $\mathcal{A}$-periodicity on the function $\boldsymbol{\Theta}^2(\bullet)$ is applied to obtain the corresponding condition on the micro-displacement at the cell boundary (the macro-position $\mathbf{y}$ is omitted for simplicity)

$$\mathbf{u}^{II}(\mathbf{z}_b + \mathbf{v}_i) - \mathbf{u}^{II}(\mathbf{z}_b) = \mathbf{u}^{*}(\mathbf{z}_b + \mathbf{v}_i) - \mathbf{u}^{*}(\mathbf{z}_b) + \boldsymbol{\Theta}^1(\mathbf{z}_b)\boldsymbol{:}\boldsymbol{\kappa}\mathbf{v}_i \qquad \mathbf{z}_b \in C_i, \quad i=1,2\,. \tag{22}$$

The boundary conditions referred to the vertical side C_1 and horizontal side C_2 are written in components in the following form, respectively:

$$
\begin{aligned}
u_i^{II}\left(z_1^+\right)-u_i^{II}\left(z_1^-\right)&=u_i^*\left(z_1^+\right)-u_i^*\left(z_1^-\right)+\theta_{i11}^{1+}d_1\kappa_{111}+\theta_{i12}^{1+}d_1\kappa_{112}+\theta_{i21}^{1+}d_1\kappa_{211}+\theta_{i22}^{1+}d_1\kappa_{221},\\
u_i^{II}\left(z_2^+\right)-u_i^{II}\left(z_2^-\right)&=u_i^*\left(z_2^+\right)-u_i^*\left(z_2^-\right)+\theta_{i11}^{1+}d_2\kappa_{112}+\theta_{i12}^{1+}d_2\kappa_{122}+\theta_{i21}^{1+}d_2\kappa_{212}+\theta_{i22}^{1+}d_2\kappa_{222},
\end{aligned}
\tag{23}
$$

where the notation $z_i^{\pm}=\pm d_i/2,\quad i=1,2$ and $\theta_{hkl}^{1+}=\theta_{hkl}^{1}\left(z_i^+\right)$ is assumed.

The corresponding micro-displacement field $\mathbf{u}^{II}\left(\mathbf{y},\mathbf{z}\right)$ is obtained by a FE analysis of the unit cell and, by the basic assumptions (4), (5), (8), (9), the unknown functions $\theta_{iklp}^{2}\left(\mathbf{z}\right)$ can be obtained by solving the system of linear equations

$$
\kappa_{klp}\theta_{iklp}^{2}\left(\mathbf{z}\right)=u_i^{II}\left(\mathbf{z}\right)-u_i^{*}\left(\mathbf{z}\right)-\theta_{ikl}^{1}\left(\mathbf{z}\right)\kappa_{klp}z_p\,,
\tag{24}
$$

where the functions at the r.h.s. are known from the previous analysis.

The elastic moduli of the second-order continuum are evaluated in the unit cell with reference to the macro-strain vectors $\underline{E}=\left\{H_{11}\quad H_{22}\quad H_{12}+H_{21}\right\}^{\mathrm{T}}$ and $\underline{\kappa}=\left\{\kappa_{111}\quad\kappa_{222}\quad\kappa_{122}\quad\kappa_{211}\quad\kappa_{121}\quad\kappa_{212}\quad\kappa_{112}\quad\kappa_{221}\right\}^{\mathrm{T}}$. The Hill-Mandel macro-homogeneity condition is applied $\mathscr{E}_M=\mathscr{E}_m$, where $\mathscr{E}_M$ is the macro-strain energy at a point **y** of the homogenized continuum assume in the following quadratic form

$$
\mathscr{E}_M\left(\underline{E},\underline{\kappa}\right)=\frac{1}{2}\left\{\underline{E}^{\mathrm{T}}\quad\underline{\kappa}^{\mathrm{T}}\right\}\begin{bmatrix}\underline{\underline{C}} & \underline{\underline{Y}}\\ \underline{\underline{Y}}^{\mathrm{T}} & \underline{\underline{S}}\end{bmatrix}\begin{Bmatrix}\underline{E}\\ \underline{\kappa}\end{Bmatrix},
\tag{25}
$$

$\underline{\underline{C}}$, $\underline{\underline{Y}}$ and $\underline{\underline{S}}$ being the sub-matrices of the second-order elastic stiffness matrix and $\mathscr{E}_m=\dfrac{1}{2A}\displaystyle\int_A\underline{\varepsilon}^{\mathrm{T}}\underline{\underline{C}}^{m}\underline{\varepsilon}\mathrm{d}a$ is the mean value of the micro-strain energy over the unit cell. According to the kinematic assumptions from the previous Section and referring to the representation of the micro-displacement field given in (10), the micro-strain field $\underline{\varepsilon}=\left\{\varepsilon_{11}\quad\varepsilon_{22}\quad 2\varepsilon_{12}\right\}^{\mathrm{T}}$ in the heterogeneous cell may be written in the following linear form

$$
\underline{\varepsilon}=\underline{\underline{B}}^{E}\left(\mathbf{z}\right)\underline{E}+\underline{\underline{B}}^{\kappa}\left(\mathbf{z}\right)\underline{\kappa}\,,
\tag{26}
$$

$\underline{\underline{B}}^{E}\left(\mathbf{z}\right)$ and $\underline{\underline{B}}^{\kappa}\left(\mathbf{z}\right)$ being matrices depending on the functions $\theta_{ikl}^{1}\left(\mathbf{z}\right)$ and $\theta_{iklp}^{2}\left(\mathbf{z}\right)$, i.e. on the microstructure of the unit cell. As a consequence the mean value of the micro-strain energy turns out to be a quadratic form in the variables $\underline{E}$, $\underline{\kappa}$ and may be compared with the macro-strain energy (25) in order to obtain the sub-matrices

$$
\underline{\underline{C}}=\frac{1}{A}\int_A\underline{\underline{B}}^{E\mathrm{T}}\underline{\underline{C}}^{m}\underline{\underline{B}}^{E}\mathrm{d}a,\quad\underline{\underline{Y}}=\frac{1}{A}\int_A\underline{\underline{B}}^{E\mathrm{T}}\underline{\underline{C}}^{m}\underline{\underline{B}}^{\kappa}\mathrm{d}a,\quad\underline{\underline{S}}=\frac{1}{A}\int_A\underline{\underline{B}}^{\kappa\mathrm{T}}\underline{\underline{C}}^{m}\underline{\underline{B}}^{\kappa}\mathrm{d}a\,.
\tag{27}
$$

The matrices $\underline{\underline{C}}$ and $\underline{\underline{S}}$ are symmetric and because of the symmetry of the second-gradient strain $\kappa_{ijk} = \kappa_{ikj}$, the additional symmetries are obtained: $S_{i5} = S_{i7}$, $S_{i6} = S_{i8}$, $Y_{i5} = Y_{i7}$ e $Y_{i6} = Y_{i8}$, $i = 1,...,8$. In general, the stiffness matrix of the second-order elastic plane model is characterised by 45 elasticities (matrix $\underline{\underline{C}}$ - 6 elasticities, matrix $\underline{\underline{S}}$ - 21 elasticities, matrix $\underline{\underline{Y}}$ -18 elasticities). In the case of centro-symmetric unit cell one obtains $\underline{\underline{Y}} = \underline{\underline{0}}$ and the first order-strain and the second-order strain are uncoupled.

Finally, the real stress $\mathbf{T}$ tensor in the homogenized medium may be obtained from the first-order stress tensor $\boldsymbol{\Sigma}$ and the second-order stress tensor $\boldsymbol{\mu}$, as shown in Section 2, represented here by the vector $\underline{\Sigma} = \{\Sigma_{11} \quad \Sigma_{22} \quad \Sigma_{12}\}^{\mathrm{T}}$ and vector $\underline{\mu} = \{\mu_{111} \quad \mu_{222} \quad \mu_{122} \quad \mu_{211} \quad \mu_{121} \quad \mu_{212} \quad \mu_{112} \quad \mu_{221}\}^{\mathrm{T}}$, respectively. From the assumption of macro-strain elastic energy, the defined stress vectors above are obtained in the following form

$$\begin{aligned} \underline{\Sigma} &= \frac{\partial \mathscr{E}_M^0}{\partial \underline{E}} = \underline{\underline{C}}\,\underline{E} + \underline{\underline{Y}}\,\underline{\kappa}, \\ \underline{\mu} &= \frac{\partial \mathscr{E}_M^0}{\partial \underline{\kappa}} = \underline{\underline{Y}}^{\mathrm{T}}\,\underline{E} + \underline{\underline{S}}\,\underline{\kappa}. \end{aligned} \tag{28}$$

A relation between the components of the macro stress vectors $\underline{\Sigma}$ and $\underline{\mu}$ and the traction vectors acting on the boundary of the unit cell is deduced from an application of the Hill-Mandel condition and is presented in Appendix A.

5. Illustrative examples

The computational homogenization proposed in this paper has been applied to the analysis of two multi-phase composites. The first is a three-phase composite with a multilayered microstructure. The second is a laminated composite made of two different elastic layers having equal thickness and characterized by continuous translational symmetry. In both composites each phase is assumed to be isotropic. The two steps of the homogenization are carried out by a FE analysis of the unit cell and the overall elastic moduli of the second-order equivalent continuum model are obtained.

To evaluate the capability of the homogenization procedure, the simple shear of a constrained two-dimensional strip having height *L* and unlimited in the horizontal direction is considered. The analysis was carried out by considering both composites and concerned

two different models: the heterogeneous model, that involves the constitutive description of each phase and is analysed under the hypothesis of standard continuum, and the homogenized continuum model, analysed as a second-order model with elastic moduli derived from computational homogenization of the unit cell. Due to the periodicity of the heterogeneous material considered along the horizontal direction, only a vertical strip of the heterogeneous model is analysed. The solution of the considered problem may exhibit boundary layer effects, the extension of which depends on the characteristic length. In case of unit cells with orthogonal symmetry axes z_1 and z_2 both the one-dimensional displacement field and the characteristic lengths are given in Appendix B. In order to assess the reliability of the second-order model, the macro-displacement and the mean rotation at some meaningful unit cells in the homogenized model are compared to the corresponding ones in the heterogeneous model. For each composite considered the comparison is carried out by considering the two orientations of the layers in the laminated composite: vertical-layer (VL) model and horizontal-layer (HL) model.

5.1 *Homogenization of a three-phase composite*

Consider a three-phase composite characterized by the unit square cell shown in figure 4a with side *d*=100mm. The constituents are assumed isotropic, perfectly bonded and in plane stress condition, with Young's modulus $E_1 = 50000$ MPa , $E_2 = 50$ MPa , $E_3 = 5000$ MPa , respectively. The Poisson ratios of the three materials equal $\nu_1 = \nu_2 = \nu_3 = 0.1$. The effective moduli obtained from the two-step second-order homogenization are given in Table 1.

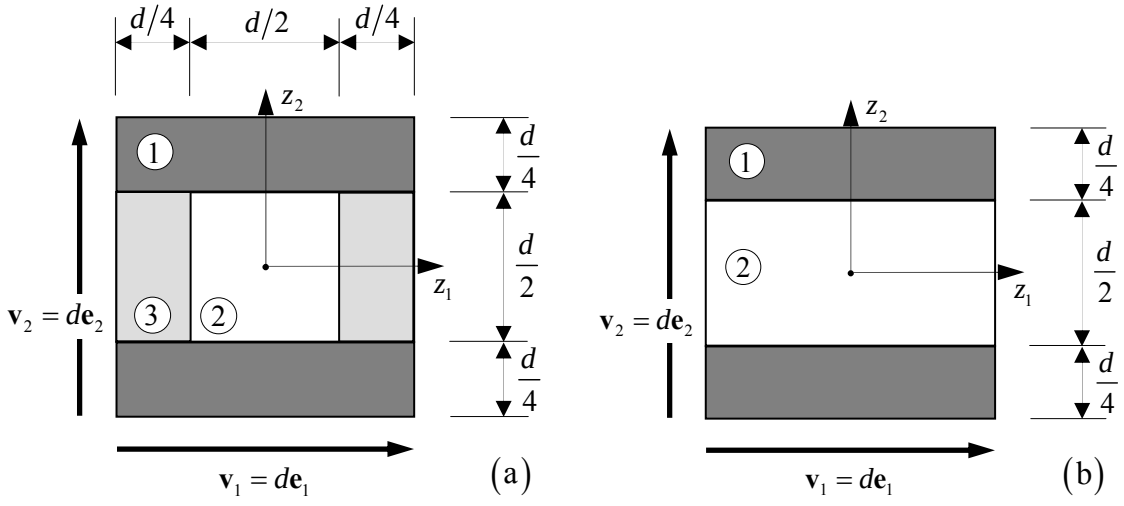

Fig. 4 Unit cell and constituents: (a) three-phase composite; (b) layered composite.

Tab.1 Elastic moduli C_{ijhk} (MPa), S_{ijhkpq} (N).

C_{1111}	C_{2222}	C_{1122}	C_{1212}
2.540E+04	4.665E+03	3.299E+02	1.238E+03

S_{111111}	S_{222222}	S_{122122}	S_{211211}	S_{121121}	S_{212212}
1.153E+05	9.090E+03	1.154E+05	4.775E+06	1.501E+07	1.838E+06

S_{111122}	S_{111212}	S_{222211}	S_{222121}	S_{122212}	S_{211121}
-4.290E+04	-1.224E+04	-1.319E+04	-4.206E+03	1.971E+05	7.048E+06

To evaluate this result, let us now consider the shear deformation of a two-dimensional strip made up of the three-phase composite. The strip has height *L*, here assumed $L = \alpha d$ (with $\alpha = 10$), and is unlimited in the horizontal direction. The periodicity of the material microstructure along the horizontal direction allows us to analyse only a vertical strip of the heterogeneous model, as shown in figure 5. Two orientations of the layers in the laminated composite are considered: vertical-layer (VL) and horizontal-layer (HL). In the heterogeneous model the lower edge is considered restrained ($u_1 = 0$, $u_2 = 0$), while a horizontal displacement $\Delta = L/100$ is prescribed to the upper edge ($u_1 = \Delta$, $u_2 = 0$). The macro-displacement field in the equivalent second-order model is uniform along direction $\tilde{y}_1$ and the corresponding boundary conditions are expressed in terms of the macro-displacement and mean rotation of the cells centred on the lower edge and on the upper edge of the strip. For the unit cell centred on the lower edge, at the origin of the axes $(\tilde{x}_1, \tilde{x}_2)$, a continuous extension of the micro-displacement field have to be considered on the lower portion of the cell, below the axis $\tilde{x}_2 = 0$, and the resulting micro-displacement field must be compatible with the boundary condition $u_2 = 0$ prescribed at points $\tilde{x}_2 = 0$ on the lower edge of the heterogeneous model. Because the unit cells have orthogonal symmetry axes z_1 and z_2, this condition is satisfied by assuming the $\tilde{x}_2 = 0$ axis as a symmetry axis: the component u_2 is an odd function of $\tilde{x}_2$ and the component u_1 is an even function. Accordingly, the vertical component of the macro-displacement and the mean rotation of the unit cell centred at the lower edge turns out to be vanishing; the same result is obtained for the macro-rotation in the Cosserat continuum evaluated according to [6]. A similar condition applies to the upper edge of the strip. Then, the boundary

conditions in the second-order model in the reference $(\tilde{y}_1, \tilde{y}_2)$ are: displacement and rotation restrained at the lower edge and displacement prescribed at the top edge with rotation restrained. Inversely, from these conditions applied to equations (4, 5, 8, 9) a micro-displacement field satisfying condition $u_2 = 0$ at the upper and lower edges is obtained.

A different interpretation of these boundary conditions may be given by considering the strip as a part of an infinite periodic composite with period of material *d* and subjected to a system of forces which is also periodic along the $\tilde{y}_2$ axis but having a larger period $2L = \alpha d$ $(\alpha \gg 1)$. These forces are uniformly applied at points on the lines of action parallel to the $\tilde{y}_2$ axis, located at distance *L* along the $\tilde{y}_2$ axis with alternating direction. Thus the unlimited domain is found in similar conditions to those considered in the asymptotic homogenization techniques [1] [2] and [4]. Here the mean rotation and the Cosserat macro-rotation are odd functions, symmetric with respect to points on the axes of symmetry of the system, i.e. the axes along which the regular forces are applied, and vanish at them. Conversely, the horizontal component of the macro-displacement is an even function with respect to the axis of symmetry.

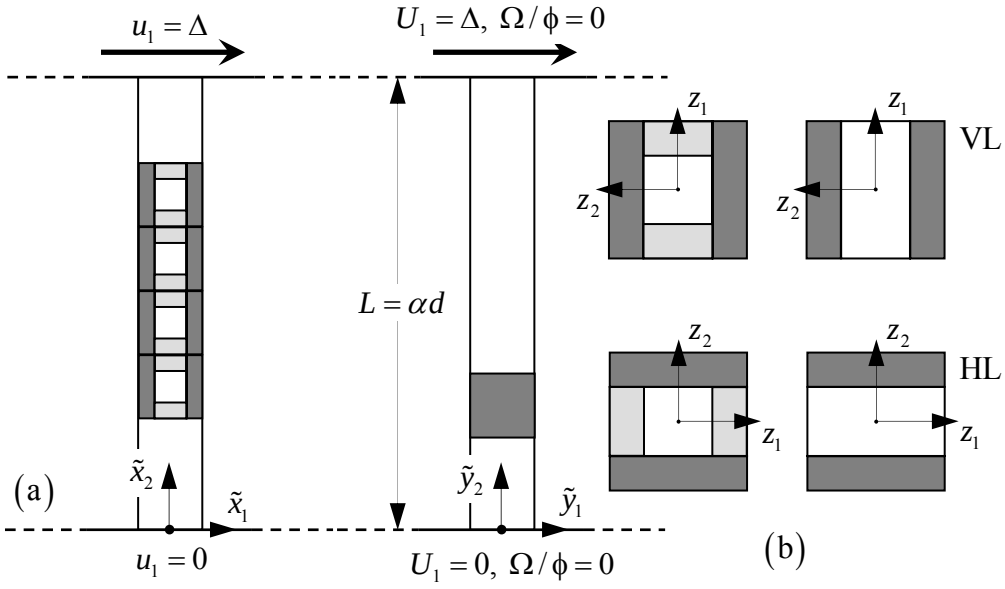

Fig. 5 . Shear of a heterogeneous strip: (a) heterogeneous model; (b) homogenized model and unit cell.

The solution to the heterogeneous problem is computed via FE, while the solution to the homogenized problem is given in Appendix B. The prescribed boundary conditions on the

homogenized second-order model determine a boundary layer effect whose thickness depends on the characteristic lengths introduced in Appendix B. The characteristic lengths associated to the shear and to extensional strain along directions z_1 and z_2 take the form

$$\lambda_{Sh-1}=\sqrt{\frac{S_{211211}}{C_{1212}}},\quad \lambda_{Sh-2}=\sqrt{\frac{S_{122122}}{C_{1212}}},\quad \lambda_{Ext-1}=\sqrt{\frac{S_{111111}}{C_{1111}}},\quad \lambda_{Ext-2}=\sqrt{\frac{S_{222222}}{C_{2222}}}, \tag{29}$$

respectively, and the numerical values for the considered unit cell are given in Table 2.

Tab.2 Characteristic lengths (mm) of the homogeneous second-order model.

$\lambda_{Sh-1}^{2\mathrm{nd}}$	$\lambda_{Sh-2}^{2\mathrm{nd}}$	$\lambda_{Ext-1}^{2\mathrm{nd}}$	$\lambda_{Ext-2}^{2\mathrm{nd}}$
62.1	9.7	2.1	1.4

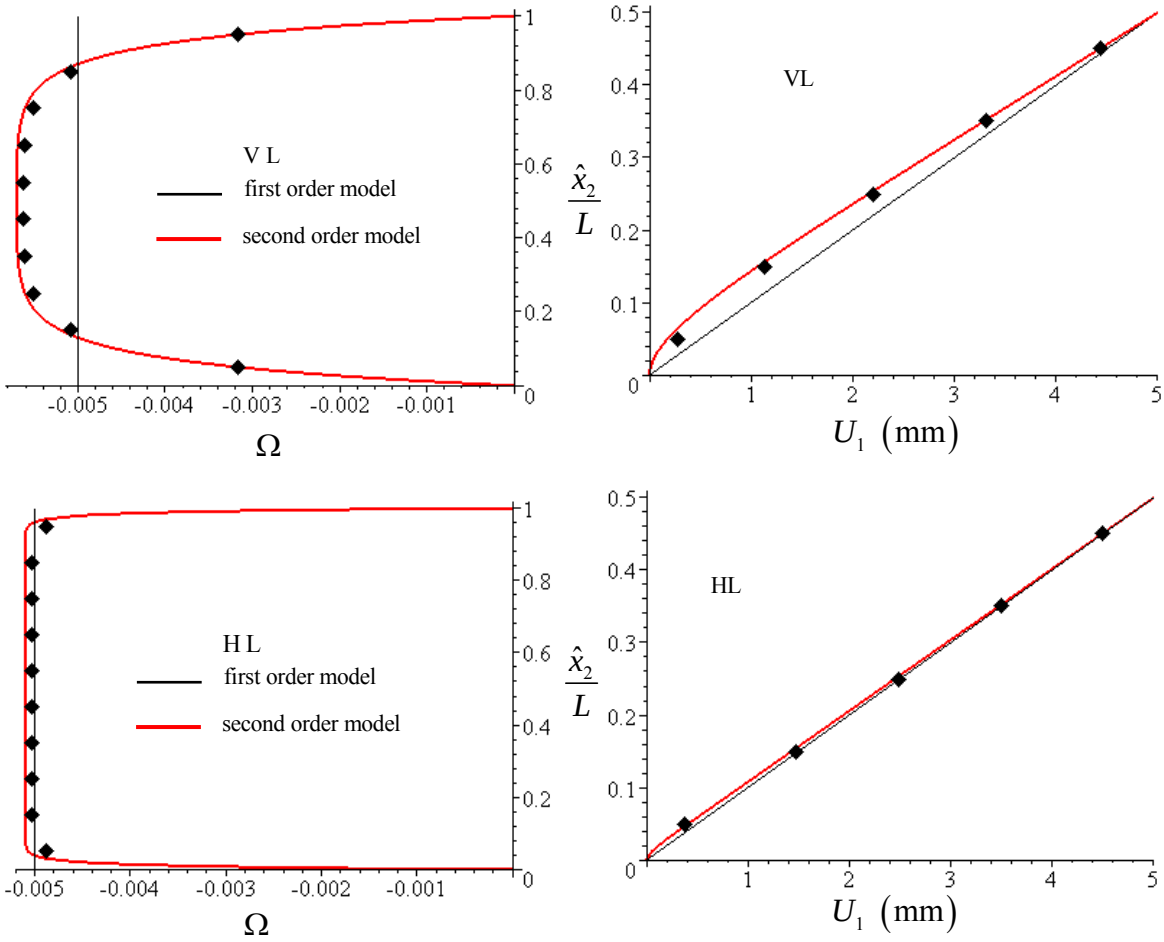

Fig. 6 Boundary shear layer problem: macro rotation and horizontal displacement at the unit cells from the heterogeneous model (diamonds) compared with the macro rotation and horizontal displacement in the homogeneous second-order model.

The numerical results obtained by the heterogeneous VL and HL models are shown in the diagrams of figure 6 as diamonds representing the mean rotation Ω and of the horizontal macro-displacement U_1 evaluated through equations (14-16) of unit cells along the height of the strip (for varying the ratio x_2/L). The continuous red lines in the diagrams represent the corresponding results from the homogenized second-order model and the black lines the results from the first-order model, respectively. While the rotation is displayed on the full height of the strip, the macro-displacement, that is antisymmetric with respect to the mid-height, is displayed on the half height only to provide a better graphical resolution. From these diagrams a good agreement is observed between the results obtained by the second-order model and the heterogeneous model for both the cases of vertical layers and horizontal layers. Moreover, in the case of HL model the width of the boundary layer appears to be negligible in comparison with the case of VL model.

The distribution of the micro-shear stress component σ_{12}, that is more significant in the VL model, is analysed in the unit cell centred on $\tilde{x}_2 = \tilde{y}_2 = 150$ mm with reference to the results form the heterogeneous model and from the equivalent homogeneous one. In figure 7.a the map of the stress component obtained by the numerical analysis of the heterogeneous model is plotted; while the corresponding map obtained by localization analysis from the second-gradient continuum is shown in figure 7.b. The contribution due the second-order strain component $\kappa_{211} = \partial^2 u_2 / \partial y_1^2$ is about 7% of the total and is shown in the map of figure 7.c.

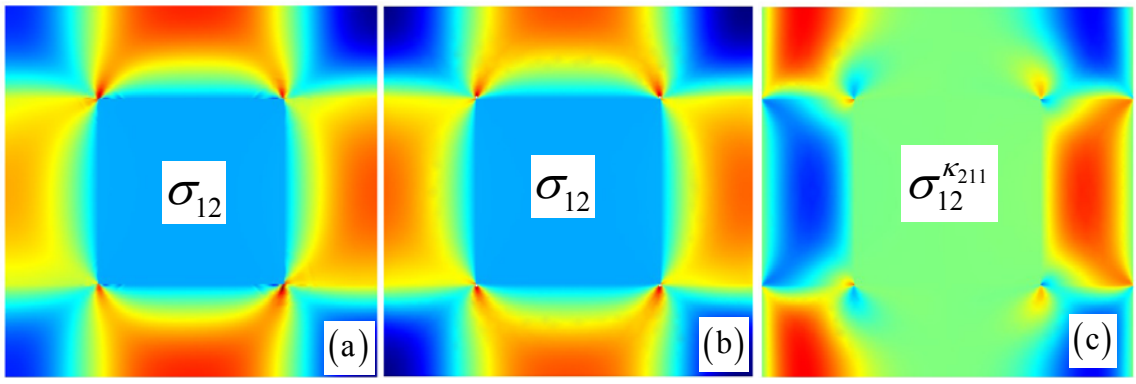

Fig. 7 Micro-shear stress component σ_{12} in the RVE at $\tilde{x}_2 = \tilde{y}_2 = 150$ mm: (a) values from the heterogeneous model; (b) values from the second-order model after localization; (c) contribution from the second-order model due the second order strain κ_{211}.

Finally, the values of the overall shear stiffness $G^* = \Sigma_{12}/(\Delta/L)$ of the strip for the vertical layer VL model provided by the different models are: (a) heterogeneous model (FE solution) G^*_{fem}=1395 MPa ; (b) first-order homogenized model G^*_C=C_{1212} =1238 MPa ; (c) second-order homogenized model G^*_{2nd}=1414 MPa . The percentage error from solution (b) with respect to (a) is -11%, while from solution (c) with respect to (a) is +1.3%. In case of horizontal layer HL one obtains: (a) G^*_{fem}=1247 MPa ; (b) G^*_C=C_{1212} =1238 MPa ; (c) G^*_{2nd}=1263 MPa . The percentage error from solution (b) with respect to (a) is -0.7%, while from solution (c) is +1.3%. These results show a different qualitative behaviour between the vertical layer model and the horizontal layer model that can be better understood by considering the following example.

5.2 *Two-phase laminated composite*

Consider now the two-phase laminated composite consisting of perfectly bonded isotropic elastic layers arranged periodically and having equal thickness $d/2 = 0.5$ mm , already analysed by Forest and Sab [6]. The layered composite is assumed in plane strain condition and Young's modulus and the Poisson ratio of the layers are denoted by $E_1 = 210000$ MPa , $\nu_1 = 0.3$, $E_2 = 1000$ MPa , $\nu_2 = 0.49$, respectively. The square unit cell shown in figure 4.b is considered having size $d = 1$ mm .

Because of the continuous translational symmetry along z_1 axis of the unit cell the functions $\theta^1_{ijk}(\mathbf{z})$ from the first-order homogenization satisfy the following boundary conditions:

$$\begin{aligned}
&\theta^1_{111}(\mathbf{z}) = \theta^1_{122}(\mathbf{z}) = \theta^1_{212}(\mathbf{z}) = \theta^1_{221}(\mathbf{z}) = 0, \qquad \mathbf{z} \in C \\
&\theta^1_{211}(\mathbf{z}) = \theta^1_{222}(\mathbf{z}) = \theta^1_{112}(\mathbf{z}) = \theta^1_{121}(\mathbf{z}) = 0, \qquad \mathbf{z} \in C_2 \\
&\int_{C_1} \theta^1_{211}(\mathbf{z})\,\mathrm{d}s = \int_{C_1} \theta^1_{222}(\mathbf{z})\,\mathrm{d}s = \int_{C_1} \theta^1_{112}(\mathbf{z})\,\mathrm{d}s = \int_{C_1} \theta^1_{121}(\mathbf{z})\,\mathrm{d}s = 0 \ ,
\end{aligned} \tag{30}$$

showing that the sides of the unit cells parallel to the layers (C_2) do not warp when first-order macro-strain are prescribed on the unit cell. As a consequence the displacement boundary conditions to be applied on the micro-displacement field $\mathbf{u}^{II}(\mathbf{y},\mathbf{z})$ in the second step of the homogenization process are written according to equations (23) and (29):

- boundary C_1

$$\begin{aligned} u_1^{II}\left(z_1^+\right)-u_1^{II}\left(z_1^-\right)&=u_1^*\left(z_1^+\right)-u_1^*\left(z_1^-\right)+\theta_{121}^{1+}\kappa_{211}d+\theta_{112}^{1+}\kappa_{112}d,\\ u_2^{II}\left(z_1^+\right)-u_2^{II}\left(z_1^-\right)&=u_2^*\left(z_1^+\right)-u_2^*\left(z_1^-\right)+\theta_{211}^{1+}\kappa_{111}d+\theta_{222}^{1+}\kappa_{212}d, \end{aligned} \tag{31}$$

- boundary C_2

$$\begin{aligned} u_1^{II}\left(z_2^+\right)-u_1^{II}\left(z_2^-\right)&=u_1^*\left(z_2^+\right)-u_1^*\left(z_2^-\right),\\ u_2^{II}\left(z_2^+\right)-u_2^{II}\left(z_2^-\right)&=u_2^*\left(z_2^+\right)-u_2^*\left(z_2^-\right), \end{aligned} \tag{32}$$

where the notations $z_i^{\pm}=\pm d/2$, $i=1,2$ and $\theta_{hkl}^{1+}=\theta_{hkl}^{1}\left(z_i^+\right)$ are assumed.

Note that the second-order strain components κ_{122} and κ_{222} are not involved in the displacement boundary conditions (31) and (32), therefore they have no effect on the micro-displacement field and on the strain energy of the unit cell. By collecting the second-order strain components in the vectors $\underline{\kappa}_1=\left\{\kappa_{111}\quad\kappa_{211}\quad\kappa_{121}\quad\kappa_{212}\quad\kappa_{112}\quad\kappa_{221}\right\}^{\mathrm{T}}$ and $\underline{\kappa}_2=\left\{\kappa_{222}\quad\kappa_{122}\right\}^{\mathrm{T}}$, the micro-strain field $\underline{\varepsilon}$ in the unit cell may be written in the form

$$\underline{\varepsilon}=\underline{\underline{B}}^{E}\left(\mathbf{z}\right)\underline{E}+\underline{\underline{B}}_1^{\kappa}\left(\mathbf{z}\right)\underline{\kappa}_1, \tag{33}$$

and the mean value of micro-strain energy turns out to be a quadratic form in the variables $\underline{E}$ and $\underline{\kappa}_1$. From the Hill-Mandel condition the macro-strain energy at a point **y** of the homogenized continuum is written in a restricted quadratic form

$$\mathscr{E}_M^{\circ}\left(\underline{E},\underline{\kappa}_1\right)=\frac{1}{2}d^2\left\{\underline{E}^{\mathrm{T}}\quad\underline{\kappa}_1^{\mathrm{T}}\right\}\begin{bmatrix}\underline{\underline{C}} & \underline{\underline{0}}\\ \underline{\underline{0}} & \underline{\underline{S}}_1\end{bmatrix}\begin{Bmatrix}\underline{E}\\ \underline{\kappa}_1\end{Bmatrix} \tag{34}$$

which is independent on the components of the second gradient of the macro-displacement vector along direction z_2, i.e. the direction normal to the layers (see figure 4.a). This result is in agreement with those provided from the asymptotic homogenization techniques, as may be derived by applying the approach by Bakhvalov and Panasenko [1] and Smyshlyaev and Cherednichenko [4] or directly by the analytical solution of Boutin [2], and is justified by noting that the sides of the unit cells parallel to the layers do not warp when first-order macro-strain is prescribed on the unit cell.

The non-vanishing effective elastic moduli C_{ijhk} and S_{ijhkpq} obtained from the second-order homogenization procedure proposed here are shown in Table 3. The characteristic

lengths associated to the shear and to extensional strain along directions z_1 and z_2 take the form respectively, and the numerical values for the considered unit cell are given in Table 4. As a consequence of the independence of the macro-strain elastic energy from the components κ_{122} and κ_{222}, the characteristic lengths along the direction normal to the layers are vanishing.

Tab.3. Elastic moduli C_{ijhk} (MPa) and S_{ijhkpq} (N).

C_{1111}	C_{2222}	C_{1122}	C_{1212}
1.000E+05	1.991E+03	5.570E+02	6.684E+02

S_{111111}	S_{211211}	S_{121121}	S_{212212}	S_{111212}	S_{211121}
1.256E+02	2.0775E+03	6.204E+03	3.810E+01	7.773E-01	3.097E+03

Tab.4. Characteristic lengths (in mm) of the laminated composite.

λ^{2nd}_{Sh-1}	λ^{2nd}_{Sh-2}	λ^{2nd}_{Ext-1}	λ^{2nd}_{Ext-2}
1.8	0	0.035	0

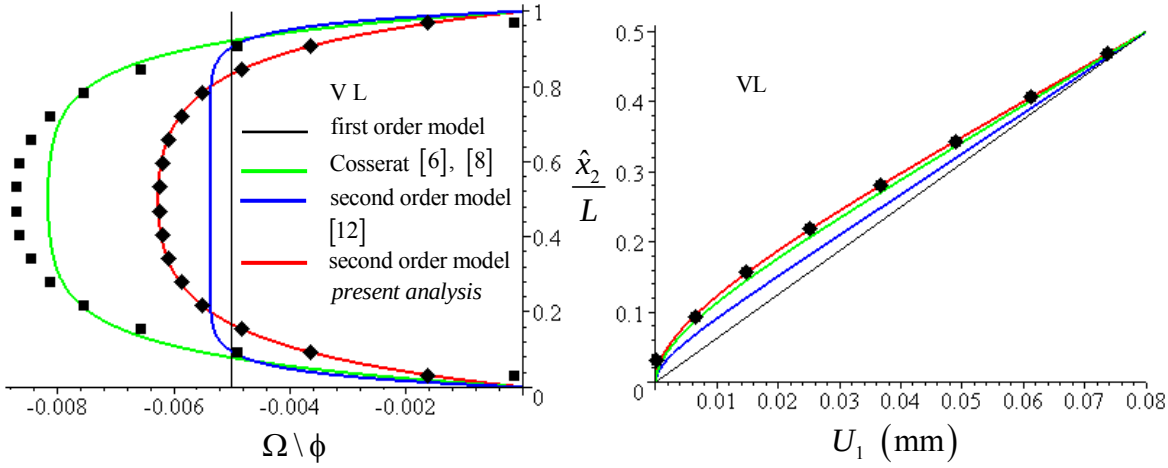

Fig. 8. Boundary shear layer problem – VL Vertical layers: mean rotation and macro-displacement from the heterogeneous model (diamonds and boxes) and from non-local models.

The boundary shear layer problem of a strip (Fig. 5.a) has been analysed with reference to two different orientations of the unit cell: vertical layer (VL) and horizontal layer (HL).

In both cases a vertical strip having height $L = \alpha d$ has been analysed, with $\alpha = 16$ and d the size of the unit cell.

The numerical results obtained by the heterogeneous model in case of vertical layers (VL) are represented in the diagrams in Figure 8, where the diamonds represent the values of the mean rotations Ω and the displacements U_1 of the unit cell according to the second-order model (equation (14-16)), while the boxes represent the values of the Cosserat rotation ϕ and the displacement of the unit cell according to the definitions given in [6]; note that diamonds and boxes in the displacement diagrams are coincident. The results from the present model are plotted in the diagrams (red line) of figure 8 together with the corresponding ones obtained by the Authors by applying the second-order homogenization procedure proposed by Kouznetsova et al. [12] and the micropolar homogenization proposed by Forest and Sab [6], [8], where ϕ is the rotation (blue and green line, respectively). The boundary conditions are those specified in the previous example: displacement and rotation restrained at the lower edge and displacement prescribed at the top edge with restrained rotation. From these diagrams, the results obtained by the second-order model appear to be in good agreement with those obtained by the heterogeneous model and a boundary shear layer is observed according to the results obtained by Forest and Sab [6]. Moreover, the macro-displacement profile in the diagram of Figure 8 is strongly reminiscent of that obtained for reinforced soil layers under shear loading evaluated on the basis of micropolar multiphase model for materials reinforced by linear inclusions proposed in [16] and [17].

The values of the overall shear stiffness provided by the different models are: (a) heterogeneous model (FE solution) G^*_{fem}=811 MPa ; (b) first-order homogenized model G^*_C=$\mathrm{C}_{1212} = 668$ MPa ; (c) second-order homogenized model G^*_{2nd}=857 MPa . The percentage error from solution (b) with respect to (a) is -17%, while from solution (c) with respect to (a) is +5.6%.

Conversely, the horizontal layer model (HL) qualitatively differs from the vertical layer model. Indeed, the response of the heterogeneous model is uniform along the strip and all cells undergo the same micro-displacement field. No boundary shear layer is obtained and the mean rotation and the macro-displacement are homogeneous and affine along the height of the strip, respectively. The first-order model turns out to be exact because lines parallel to the layers do not warp, i.e. $u_2 = 0$, a circumstance that is directly detected by the

proposed homogenization approach, which provides vanishing characteristic lengths λ_{Sh-2}^{2nd} and λ_{Ext-2}^{2nd} along direction z_2.

If a small perturbation of the layered unit cell is considered, a warping of the cell sides parallel to the layers is obtained and the boundary conditions on the lower and upper edges of the strip have to include vanishing rotation as shown in the previous example, with a resulting boundary layer effect on the mean rotation and macro-displacement. The homogenization technique proposed here may describe the continuous transition between the two different behaviours as it provides characteristic lengths in the constitutive equations that become vanishing as the perturbation tends to zero, i.e. in moving towards the layered cell, as the size of boundary shear layer. As an example, consider the cell of figure 4.a with d=1mm, elastic moduli $E_1 = 210000$ MPa, $E_2 = 1000$ MPa, $E_3 = \eta E_2$ and Poisson ratios $\nu_1 = 0.3$, $\nu_2 = \nu_3 = 0.49$, where η is a perturbation parameter with respect to the layered model ($\eta = 1$). The characteristic length λ_{Sh-2}^{2nd} is shown in the diagram of figure 9 as a function of η. In figure 10 the rotation and displacement diagrams $(\Omega,\ \phi)$ along the strip are given for a perturbation $\eta = 1.01$. The thickness of the boundary layer tends to zero as $\eta \to 1$. Finally, if the strip is considered as a portion of an unlimited domain subjected to a periodic system of forces, the rotation and the macro-displacement tend continuously as $\eta \to 1$ to a square wave function and a triangle wave function, respectively.

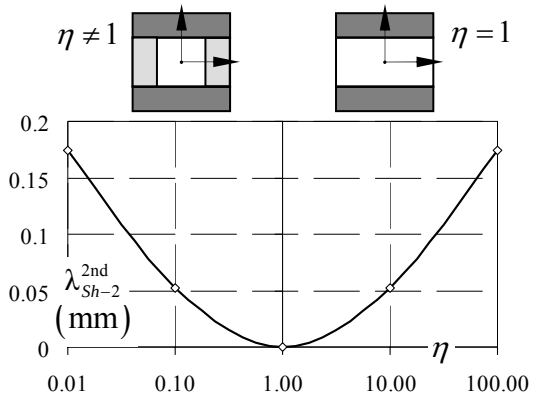

Fig.9. Characteristic length as a function of the perturbation parameter.

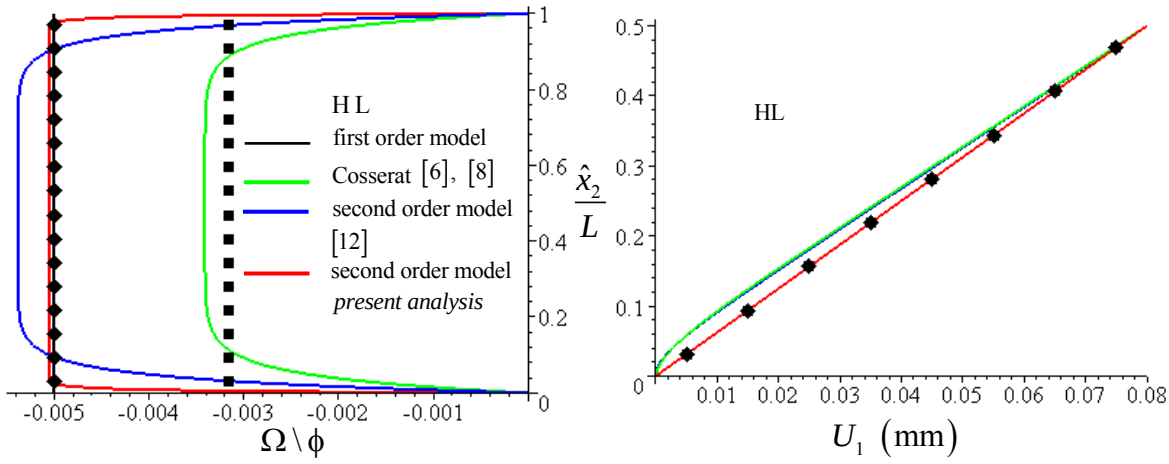

Fig.10. Boundary shear layer problem – HL horizontal layers ($\eta = 1.01$): mean rotation and macro-displacement from the heterogeneous model and from non-local models.

6. Conclusions

The proposed second-order computational homogenisation is obtained by the analysis of the unit cell representative of the heterogeneous periodic material and is based on an appropriate representation of the micro-displacement field. This field is assumed as the superposition of a local macroscopic displacement field, expressed in a polynomial form related to the macro-displacement field, and an unknown micro-fluctuation field accounting for the effects of the heterogeneities. This second contribution is represented as the superposition of two unknown functions each of them related to the first-order and to the second-order strain, respectively. This kinematical micro-macro framework guarantees that the micro-displacement field is continuous across the interfaces between adjacent unit cells and implies a computationally efficient procedure that applies in two steps. The first step corresponds to the standard homogenization, while the second step is based on the results of the first step and complete the second-order homogenization. In this sense the proposed procedure has some similarities with the methods of asymptotic homogenization because it is developed according to sequential steps; the results from the first step, i.e. the microstructural displacement fluctuation field obtained by the first-order homogenization, are applied in the second step concerning the second-order homogenization.

Two multi-phase composites, a three-phase and a laminated composite, are analysed in the examples to assess the reliability of the homogenization techniques. The overall elastic moduli and the characteristic lengths of the second-order equivalent continuum model are obtained by the computational homogenization carried out by the FE analysis of the unit

cell. Finally, the simple shear of a constrained heterogeneous two-dimensional strip made up of the considered composites is analysed by considering a heterogeneous continuum and a homogenized second-order continuum. A boundary layer effect is observed in the case of three-phase material regardless of the orientation of the microstructure with a good agreement between the results provided by the equivalent homogenized second-order model and those from the first-order heterogeneous model. For the cases where the strip is made up of the laminated composite, a boundary shear layer effect is obtained for vertical layers, an effect which is not observed for horizontal layers.

Acknowledgment

The authors acknowledge financial support of the (MURST) Italian Department for University and Scientific and Technological Research in the framework of the research MIUR Prin07 project 2007YZ3B24, *Multi-scale problems with complex interactions in Structural Engineering*, coordinated by prof. A. Corigliano.

References

[1] N.S. Bakhvalov, G.P. Panasenko, Homogenization: Averaging Processes in Periodic Media. Nauka, Moscow (in Russian). English translation in: Mathematics and its Applications (Soviet Series) 36, Kluwer Academic Publishers, Dordrecht-Boston-London, 1984.

[2] C. Boutin, Microstructural effects in elastic composites, *Int. J. Solids and Structures*, **33** ,1023-1051, 1996.

[3] N. Triantafyllidis, S. Bardenhagen, The influence of scale size on the stability of periodic solids and the role of associated higher order gradient continuum models, *J. Mechanics and Physics of Solids*, **11**, 1891-1928, 1996.

[4] V.P. Smyshlyaev, K.D. Cherednichenko, On rigorous derivation of strain gradient effects in the overall behaviour of periodic heterogeneous media, *J. Mechanics and Physics of Solids*, **48**, 1325-1357, 2000.

[5] R.H.J. Peerlings, Fleck N.A., Computational Evaluation of Strain Gradient Elasticity Constants, *Int. J. for Multiscale Computational Engineering*, **2**, 599-619, 2004.

[6] S. Forest, K. Sab, Cosserat overall modeling of heterogeneous materials, *Mech. Res. Comm.*, **25**, 449-454, 1998.

[7] F. Feyel, A multilevel finite element method (FE^2) to describe the response of highly

non-linear structures using generalized continua, *Comput. Methods Appl. Mech. Engrg.* **192**, 3233–3244, 2003.

[8] Bacigalupo A., Gambarotta L., Non-Local Computational Homogenization of Periodic Masonry, *Int. J. for Multiscale Computational Engineering*, to appear, 2010.

[9] O. van der Sluis, P.H.J. Vosbeek, P.J.G. Schreurs, H.E.H. Meijer, Homogenization of heterogeneous polymers, *Int. J. Solids and Structures*, **36**, 3193–3214, 1999.

[10] F. Bouyge, I. Jasiuk, M. Ostoja-Starzewski, A micromechanically based couple-stress model of an elastic two-phase composite, *Int. J. Solids and Structures*, **38**, 1721-1735, 2001.

[11] F. Bouyge, I. Jasiuk, S. Boccara, M. Ostoja-Starzewski, A micromechanically based couple-stress model of an elastic orthotropic two-phase composite, *European J. of Mechanics A/Solids*, **21**, 465-481, 2002.

[12] V.G. Kouznetsova, M.G.D. Geers, W.A.M. Brekelmans, Multi-scale second-order computational homogenization of multi-phase materials: a nested finite element solution strategy, *Comput. Methods Appl. Mech. Engrg*. **193**, 5525–5550, 2004.

[13] Ł. Kaczmarczyk, C. Pearce, N. Bićanić, Scale transition and enforcement of RVE boundary conditions in second-order computational homogenization, *Int. J. Numerical Methods in Engineering*, **74**, 506-522, 2008.

[14] Xi Yuan, Yoshihiro Tomita, Tomoaki Andou, A micromechanical approach of non local modelling for media with periodic microstructures, *Mech. Res. Commun.* **35**, 126–133, 2008.

[15] P. Germain, The method of virtual power in continuum mechanics. Part 2: microstructure, *SIAM J. Appl. Math.* **25** (3), 556–575, 1973.

[16] P. de Buhan, Sudret, B., Micropolar multiphase model for materials reinforced by linear inclusions. *Eur. J. Mech. A/Solids*, **19**, 669–687, 2000.

[17] P. de Buhan, G. Hassen, Multiphase approach as a generalized homogenization procedure for modelling the macroscopic behaviour of soils reinforced by linear inclusions, *Eur. J. Mech. A/Solids*, **27**, 662–679, 2008.

Appendix A

According to the Hill-Mandel assumption it is required that the surface average of the power $P_{mi} = 1/A \int_A \sigma_{ij}\dot{\varepsilon}_{ij} da$ of the internal forces in the unit cell must be equal to the power $P_{Mi} = \left(\Sigma_{ij}\dot{E}_{ij} + \mu_{pqr}\dot{\kappa}_{pqr}\right)$ of the internal forces in the homogenized continuum. By the principle of virtual power and by considering the power of the tractions acting on points of the boundary C of the unit cell (body forces are assumed vanishing) having velocity $\dot{\mathbf{u}}$ expressed according to assumptions (4-5), (8-9) one obtains

$$P_{mi} = P_{me} = \frac{1}{A}\int_C t_i \dot{u}_i ds = \frac{1}{A}\int_C t_i \left\{\dot{U}_i + \dot{H}_{ij} z_j + \frac{1}{2}\dot{\kappa}_{ipq} z_p z_q + \theta^1_{ipq}\left[\dot{H}_{pq} + \dot{\kappa}_{pqr} z_r\right] + \theta^2_{ipqr}\dot{\kappa}_{pqr}\right\} ds =$$
$$= \frac{1}{A}\left(\int_C \left(t_i z_j + t_h \theta^1_{hij}\right) ds\right)\dot{H}_{ij} + \frac{1}{A}\left(\int_C \left(\frac{1}{2} t_p z_q z_r + t_i \theta^1_{ipq} z_r + t_i \theta^2_{ipqr}\right) ds\right)\dot{\kappa}_{pqr} \quad .$$

As the Hill-Mandel condition must hold for any macro-strain rate $\dot{E}_{ij}$, $\dot{\kappa}_{pqr}$ the components of the macro stress tensors are obtained in terms of the traction acting on the unit cell boundary C in the following form

$$\begin{aligned} \Sigma_{ij} &= \frac{1}{A}\int_C \left(t_i z_j + t_h \theta^1_{hij}\right) ds, \\ \mu_{pqr} &= \frac{1}{A}\int_C \left(\frac{1}{2} t_p z_q z_r + t_i \theta^1_{ipq} z_r + t_i \theta^2_{ipqr}\right) ds. \end{aligned} \tag{A.1}$$

In the case of self-equilibrated anti-periodic traction applied in C , by noting that θ^1_{hij} , θ^2_{ipqr} are $\mathscr{A}$-periodic, it follows

$$\begin{aligned} \Sigma_{ij} &= \frac{1}{A}\int_C t_i z_j ds, \\ \mu_{pqr} &= \frac{1}{A}\int_C \left(\frac{1}{2} t_p z_q z_r + t_i \theta^1_{ipq} z_r\right) ds. \end{aligned} \tag{A.2}$$

Appendix B

With reference to Section 2, the equilibrium of an elastic body with applied tractions on its boundary and vanishing body forces may be analysed through a displacement formulation. From the compatibility equations $E_{ij} = \frac{1}{2}\left(U_{i,j} + U_{j,i}\right)$, $\kappa_{ijq} = U_{i,jq}$ and the

constitutive equation (3), the equilibrium equation (1) with $f_i = 0$ may be written in the form

$$S_{ijqhkp}U_{h,kpqj} + \left(Y_{hkijp} - Y_{ijhkp}\right)U_{h,kpj} - C_{ijhk}U_{h,kj} = 0\,. \tag{B.1}$$

These equations are simplified when applied to two-dimensional bodies having a microstructure characterized by unit cells with orthogonal symmetry axes z_1 and z_2 $\left(Y_{hkijp} = 0\right)$. Here two special cases are considered where the displacement vector is considered homogeneous along direction y_β. In the extensional problem the non vanishing component of the displacement is U_α, while in the shearing problem the non vanishing component is U_β. The differential equations related to the two problems are

$$\begin{aligned} S_{\alpha\alpha\alpha\alpha\alpha\alpha}U_{\alpha,\alpha\alpha\alpha\alpha} - C_{\alpha\alpha\alpha\alpha}U_{\alpha,\alpha\alpha} &= 0, \\ S_{\beta\alpha\alpha\beta\alpha\alpha}U_{\beta,\alpha\alpha\alpha\alpha} - C_{\alpha\beta\alpha\beta}U_{\beta,\alpha\alpha} &= 0, \end{aligned} \tag{B.2}$$

respectively, whose solution are written in the form

$$\begin{aligned} U_\alpha\left(y_\alpha\right) &= A\cosh\left(\frac{y_\alpha}{\lambda^{2\text{nd}}_{Ext-\alpha}}\right) + B\sinh\left(\frac{y_\alpha}{\lambda^{2\text{nd}}_{Ext-\alpha}}\right) + Cy_\alpha + D, \\ U_\beta\left(y_\alpha\right) &= A\cosh\left(\frac{y_\alpha}{\lambda^{2\text{nd}}_{Sh-\alpha}}\right) + B\sinh\left(\frac{y_\alpha}{\lambda^{2\text{nd}}_{Sh-\alpha}}\right) + Cy_\alpha + D, \end{aligned} \tag{B.3}$$

where $\lambda_{Ext-\alpha} = \sqrt{\dfrac{S_{\alpha\alpha\alpha\alpha\alpha\alpha}}{C_{\alpha\alpha\alpha\alpha}}}$ and $\lambda_{Sh-\alpha} = \sqrt{\dfrac{S_{\beta\alpha\alpha\beta\alpha\alpha}}{C_{\alpha\beta\alpha\beta}}}$ are the extensional and the shearing characteristic lengths, respectively, and A, B, C, D are arbitrary constants to be determined by the macroscopic boundary conditions. The non-vanishing strain components for the two problems are $E_{\alpha\alpha} = U_{\alpha,\alpha}$, $\kappa_{\alpha\alpha\alpha}$ and $E_{\alpha\beta} = \Omega_{\alpha\beta} = U_{\beta,\alpha}/2$, $\kappa_{\beta\alpha\alpha}$, respectively. Finally, the components $\mathrm{T}_{ij} = \Sigma_{ij} - \mu_{ijk,k}$ of the real stress tensor take the following form

$$T_{ij} = \delta_{ij}\left(C_{ij\alpha\alpha}E_{\alpha\alpha} - S_{ij\alpha\alpha\alpha\alpha}\kappa_{\alpha\alpha\alpha,\alpha}\right), \qquad T_{ij} = \left(1-\delta_{ij}\right)\left(2C_{ij\alpha\beta}E_{\alpha\beta} - S_{ij\alpha\beta\alpha\alpha}\kappa_{\beta\alpha\alpha,\alpha}\right), \tag{B.4}$$

where δ_{ij} is the Kronecker delta.